

SELF-FOCUSING OF LASER RADIATION IN SOLID DIELECTRICS

G. M. ZVEREV and V. A. PASHKOV

Submitted May 8, 1969

Zh. Eksp. Teor. Fiz. 57, 1128–1138 (October, 1969)

Self-focusing of the second harmonic radiation ($\lambda = 530$ nm) of a single-mode neodymium laser resulting in the formation of filamentary fractures in glasses, sapphire, and ruby is investigated. Compression of the laser beam prior to filamentary fraction was observed. The threshold radiation powers leading to formation of filamentary defects in materials with different absorption are measured as functions of the conditions of laser-radiation focusing on the samples. The rate of "growth" of the filamentary fractures towards the laser beam ($\sim 10^8$ cm/sec) is determined. The dependence of the filament lengths on the incident power is investigated. The magnitude of nonlinear changes in the refraction index n_2 is estimated on the basis of the experimental results, and possible self-focusing mechanisms in solid dielectrics are discussed.

INTRODUCTION

FOR many years, the phenomenon of self-focusing of laser radiation^[1-3] has been attracting the attention of many investigators. In most experiments, this phenomenon was investigated in liquids (see, for example,^[4]). At the same time, self-focusing of laser radiation takes place also in many solid dielectrics. In such materials as glass^[5], quartz, ruby, leucosapphire, or nonlinear crystals^[6,7], the passage of a laser beam gives rise to characteristic filamentary damage, which can be explained only as a result of self-focusing. Similar damage can be observed directly in the active elements of Q-switched lasers, namely ruby and neodymium glass^[7]. Self-focusing in laser materials can influence also the formation of the laser radiation field, and determine the limiting endurance of these materials under the action of powerful optical radiation.

It was shown in^[8] that the filamentary damage observed in solid dielectrics is not connected with the waveguide propagation of light in the medium. This damage occurs when the region in which the light beam collapses as a result of the increase of the refractive index of the medium propagates in the medium during the time of the laser pulse in a direction opposite to the incident radiation.

We report here further investigations of the self-focusing of laser radiation in solid dielectrics, namely transparent and colored glasses, leucosapphire, and ruby. We show that the appearance of filamentary damage is preceded by light-beam contraction caused by the self-focusing. We measure the threshold laser radiation power, at which filamentary damage occurs in materials with different absorption, as a function of the conditions for the focusing of the laser radiation in the samples. We studied the dynamics of development of the filamentary damage, determine the rate of "growth" of the filament-like damage in a direction opposite to the incident beam. We investigate the dependence of the length of the filaments on the incident power.

On the basis of the experimental results, we estimate the values of the nonlinear additions to the refractive index of the medium in the field of the light wave, and consider possible mechanisms of self-focusing in the investigated materials.

EXPERIMENTAL PROCEDURE

The self-focusing investigations were carried out in transparent dielectrics—optical glass K-8 and leucosapphire. We also investigated colored materials—glass ZhS-11, sapphire crystals with small additions of chromium, and ruby crystals. In the experiments we used second-harmonic radiation of a Q-switched neodymium laser operating with one transverse mode. The second-harmonic radiation ($\lambda = 0.53 \mu$) led to the formation of longer filamentary flaws with smaller threshold than the radiation from a neodymium laser ($\lambda = 1.06 \mu$). In this case the filaments were not accompanied by strong cracking of the material. The single-mode laser operation made it possible to obtain one filamentary flaw per flash with good reproducibility of the results.

The laser consisted of a generator and one amplifier with active elements of LGS-5 glass, measuring 10 mm in diameter and 130 mm in length. The concentric resonator of the generator was made up of a spherical dielectric mirror and a flat glass substrate. The Q switch was a phototropic liquid. To obtain stable generation on one transverse mode, a diaphragm of 2.0 mm diameter was placed in the resonator.

The experimental setup is shown in Fig. 1. The radiation from the master generator 1 was amplified in amplifier 2 and directed to KDP crystal 3 to obtain the second harmonic. The SZS-21 filter 4 absorbed the radiation of the fundamental frequency of the neodymium laser, while the neutral filters 5 made it possible to vary the energy of the harmonic. The radiation passed by the filters was focused by a lens 6 into the interior of the investigated polished samples 7. Part of the

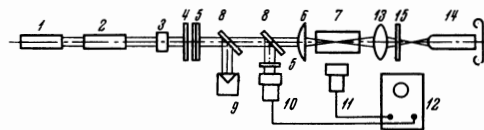


FIG. 1. Diagram of experimental setup. 1 — Neodymium-glass laser ($\lambda = 1.06 \mu$), 2 — amplifier, 3 — KDP crystal, 4 — SZS-21 filter, 5, 15 — neutral filters, 6 — focusing lens, 7 — investigated sample, 8 — glass plates, 9 — calorimeter, 10, 11 — FÉK-09 photodiodes, 12 — S1-11 oscilloscope, 13 — photographic objective, 14 — microscope with camera.

radiation was diverted by glass plates 8 to a calorimeter 9 in order to measure the energy and to a photodiode 10 in order to trigger the sweep of the S1-11 oscilloscope 12. A high-speed FÉK-09 photodiode 11 was used to register the scattered laser radiation on the developing filamentary flaw. The field distribution of the laser radiation was investigated with the aid of photographic lens 13 and a microscope with photographic camera 14, placed behind the output surface of the sample. The neutral filters 15 made it possible to obtain photographic images of normal density.

The energy of the neodymium-laser harmonic reached 0.02 J at a pulse duration of approximately 10 nsec. The beam diameter in the plane of the lens was 1.5 mm. The length of the filamentary flaw following application of the total radiation power and using a focusing lens with $f = 110$ cm fluctuated for different samples from 15 to 30 mm. The longest filaments in the colored glass ZhS-11 greatly exceeded the focal length

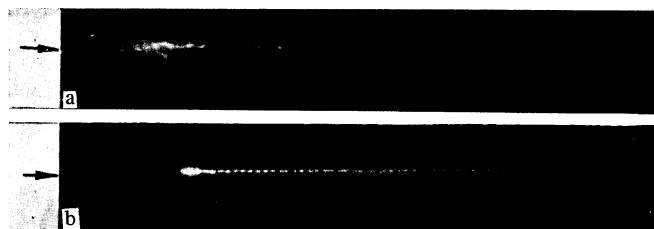


FIG. 2. Filamentary flaw: a – in glass, b – in sapphire. The arrow shows the direction of propagation of the laser beam. Magnification 50X.

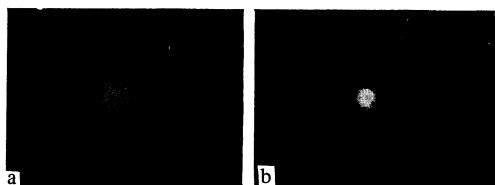


FIG. 3. Field distribution at the focus of the lens: a – $P = 0.5P_{thr}$, b – $P = 0.9P_{thr}$. Magnification 65X.

of the lens. The diameter of the filament at the region of the focus of the lens was approximately 5μ , increasing to $10\text{--}12 \mu$ towards the end the diameter increased, and the filament usually terminated in a crack measuring $0.1\text{--}0.5$ mm. As a rule, practically continuous filamentary flaws were observed (Fig. 2a).

However, in many cases intermittent filaments with a clearly pronounced periodic structure were observed. The most distinct periodicity (with a distance of ap-

proximately 20μ between the flaws) was observed in leucosapphire crystals (Fig. 2b). This character of the damage may be connected with the high-frequency modulation of the laser pulse, with approximate frequency 5×10^{10} Hz, due to beats of the neighboring axial modes.

Filamentary flaws induced by the fundamental frequency of the neodymium laser reached up to 20μ in diameter and was accompanied by appreciable cracking of the material.

2. CHANGE OF TRANSVERSE LASER BEAM STRUCTURE PRECEDING THE FILAMENTARY DAMAGE

The $0.53\text{-}\mu$ radiation was focused with a lens of $f = 40$ cm into a sample of ZhS-11 glass. Over the length of the sample ($l = 60$ mm), the cross section of the laser beam remained practically constant (at low intensities) at about 10^{-2} cm. The ZhS-11 glass has the lowest threshold of filamentary damage among all the investigated materials, making it possible to use long-focus lenses. Under such conditions, it is possible to observe most clearly the contraction of the light beam.

Figure 3 shows photographs of the transverse cross section of the laser beam passing through the sample at power levels close to the threshold of the filamentary damage P_{thr} . At a power $P \leq 0.5P_{thr}$, the radiation field has a Gaussian character (Fig. 3a). Raising the power to $0.9P_{thr}$ leads to the appearance of a bright central region in the beam, with diameter $30\text{--}50 \mu$. At a power corresponding to the threshold of the filamentary damage, the diameter of the bright region is close to the diameter of the filament (approximately 10μ).

These results show that filamentary damage in solid dielectrics is directly connected with the phenomenon of self-focusing of the laser radiation. We note that the action of a single-mode laser leads to the appearance of one central spot in the distribution of the radiation field, and consequently, to one damage filament. At the same time, in the case of a multimode regime, a number of filaments per flash is produced^[6,7]: the most intense regions of the laser beam are focused separately into filaments.

3. THRESHOLDS OF FILAMENTARY DAMAGE. DEPENDENCE OF THE FILAMENT LENGTH ON THE RADIATION POWER

We measured the threshold of filament-like damage with a lens ($f = 10$ cm) at a radiation wavelength 0.53μ in the K-8 and ZhS-11 glass, in sapphire with varying absorption, and in ruby. The table lists the thresholds for the investigated materials, and also the values of the absorption coefficient κ at the generation wavelength.

The lowest threshold was observed in colored glass

Material	κ, cm^{-1}	P_{thr}, MW	P_{cr}, MW	n_2 from threshold measurements	n_2 from measurements of filament lengths	n_2 , theory [12, 13]
K-8 glass	$\sim 10^{-3}$	0.3	0.7	$3 \cdot 10^{-14}$	$1.6 \cdot 10^{-14}$	$\left\{ \begin{array}{l} 1.5 \cdot 10^{-14} \\ \text{(striction)} \\ 1.0 \cdot 10^{-14} \\ \text{(thermal)} \\ 1.0 \cdot 10^{-18} \\ 2 \cdot 10^{-18} \end{array} \right.$
Leucosapphire	$1 \cdot 10^{-2}$	0.5			$0.6 \cdot 10^{-18}$	
Sapphire	$2.3 \cdot 10^{-2}$	0.25	0.5	$0.6 \cdot 10^{-18}$	$1.2 \cdot 10^{-18}$	
Ruby	1.5	0.14				
ZhS-11 glass	$4.2 \cdot 10^{-2}$	0.1	0.15	$1.7 \cdot 10^{-18}$	$4 \cdot 10^{-18}$	

ZhS-11. In sapphire, the threshold dropped with increasing absorption coefficient. In a ruby crystal with absorption coefficient $\kappa = 1.5 \text{ cm}^{-1}$ at a wavelength 0.53μ , the threshold depended on the position of the focal region in the sample. If the distance from the input surface of the sample to the focus l_f exceeds $1/\kappa$, then the threshold in ruby is higher than in sapphire, owing to the strong absorption in the sample. In the opposite case, when $l_f < 1/\kappa$, the threshold in ruby is lower than in leucosapphire. The table lists the value of the threshold in ruby for $l_f = 0.5 \text{ cm}$. At the same time, the thresholds in materials with small absorption ($l_f \ll 1/\kappa$) remain practically unchanged when l_f varies in a wide range.

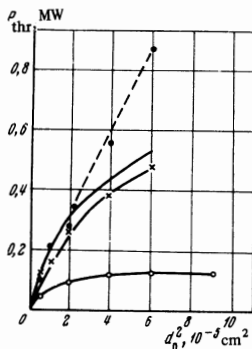


FIG. 4

FIG. 4. Dependence of threshold power of formation of filamentary damage, P_{thr} , on the square of the diameter of the focal spot, d_0^2 . ○ — ZhS-11 glass, × — sapphire, ● — K-8 glass.

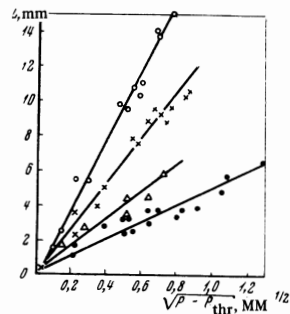


FIG. 5

FIG. 5. Dependence of filament length L on the radiation power. ○ — ZhS-11 glass, Δ — leucosapphire, × — sapphire ($\kappa = 2.3 \times 10^{-2} \text{ cm}^{-1}$), ● — K-8 glass.

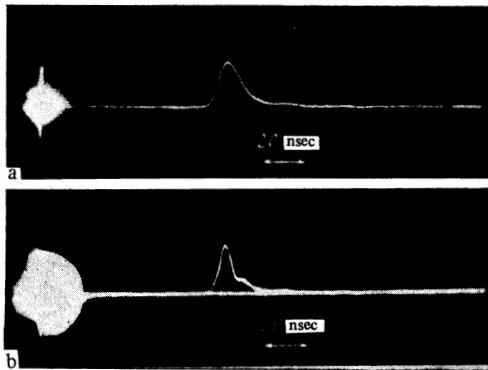


FIG. 6. Oscillograms of laser pulse passing through a sample at a power below threshold (a) and a power corresponding to the threshold (b). Sweep rate 20 nsec per division.

It follows from the table that in both glass and sapphire the thresholds of the filamentary damage decrease with increasing absorption coefficient.

We measured the dependence of the thresholds of filamentary damage in the glasses K-8 and ZhS-11 and in sapphire with absorption coefficient $2 \times 10^{-2} \text{ cm}^{-1}$ on the diameter d_0 of the focal spot. d_0 ranged from 2×10^{-3} to $8 \times 10^{-3} \text{ cm}$, when lenses with focal lengths from 4.8 to 19 cm were used. As seen from Fig. 4, for

the glass K-8 the threshold power $P_{thr} \sim d_0^2$, whereas for ZhS-11 and sapphire the dependence of P_{thr} on d_0 is closer to linear.

We investigated also the dependence of the length of the filamentary flaws in K-8 and ZhS-11 glasses and in sapphire crystals with different absorption on the laser radiation power. The lengths of the filaments, using a focusing lens with $f = 10 \text{ cm}$, ranged from 0.5 mm at the threshold to 10–20 mm in sapphire and K-8 glass, and up to 30 mm in ZhS-11 glass at the total radiation power (2 MW).

Figure 5 shows the dependence of the lengths of the filaments on the quantity $(P - P_{thr})^{1/2}$, where P is the radiation power. This dependence is extrapolated by straight lines. The largest slope is observed for the glass ZhS-11.

4. DISTORTION OF LASER-PULSE WAVEFORM FOLLOWING OCCURRENCE OF FILAMENTARY DAMAGE

To determine the inertia of the development of self-focusing in solid dielectrics, we investigated the waveform of a laser pulse passing through the ZhS-11 glass and sapphire samples at a power close to the threshold of the filamentary damage. The radiation passing through the sample was directed to an FÉK-09 photodiode and registered with an S1-11 oscilloscope with 2 nsec time resolution.

Figure 6 shows oscillograms of laser pulses at a power 10–20% below the damage threshold (Fig. 6a) and at a power slightly exceeding the threshold (Fig. 6b). The distortion of the pulse, observed in Fig. 6b, is due to absorption and scattering of the beam, which has been compressed by self-focusing, by the produced filamentary flaw. If the radiation is attenuated by a neutral filter in such a way that no self-focusing of the beam occurs, and the beam is passed again through a region of the sample where filamentary flaw is already present, then no distortion of the laser waveform will be observed. At low radiation intensity, a thin filamentary flaw (5–10 μ diameter) has little effect on the propagation of the light beam through a focal region of about 50 μ diameter. The time during which the change in the pulse waveform is observed corresponds to the time of existence of the compressed state of the light beam, when its diameter is close to the diameter of the filamentary flaw.

As seen from the oscillogram on Fig. 6b, the distortion appears after the maximum of the laser pulse (2–3 nsec later) and is observed practically to its end. From the considerable depth of the dip in the pulse it follows that a large section of the beam cross section is involved, carrying up to 70% of the power. The delay of the dip relative to the maximum of the laser pulse offers evidence that the mechanisms that lead to self-focusing are subject to inertia.

5. DYNAMICS OF DEVELOPMENT OF FILAMENT-LIKE DAMAGE

As shown in^[8], filamentary damage in solid dielectrics develops in a direction opposite to the incident radiation as a result of motion, in this direction, of a region of collapse of the light beam. This is due to the

growth of the refractive index of the medium in the field of the light wave during the laser pulse.

We have investigated the dynamics of the development of filamentary damage and determined the rate of motion of the filament in a direction opposite to the laser beam. 0.53- μ radiation at full power was focused into a ZhS-11 glass sample, in which the filamentary flaws are longest. An FÉK-09 photodiode located near the sample, perpendicular to the laser beam (Fig. 1), registered the laser radiation scattered from the developing filamentary flaw. After each flash, the sample was moved 1–2 mm in a direction perpendicular to the light-beam axis. The signal from the photodiode was fed to an S1-11 oscilloscope (the resolution of the oscilloscope with the amplifier was 4 nsec). Figure 7a shows an oscillogram of the pulse scattered by the filamentary flaw. The oscillogram of Fig. 7b shows the laser pulse scattered only by the ends of the filament. Its central part was covered with an opaque screen 15 mm wide, and the ends projected approximately 5 mm from each side of the screen. It is seen from this oscillogram that the damage in the filament occurs during the time of the laser pulse, and that the delay between the time of formation of the start and the end of the filamentary flaw is 8–10 nsec, corresponding to a filament "growth" rate $(1.5-2) \times 10^8$ cm/sec. By moving the screen, it is easy to show that the filament is generated in the focal region of the lens and develops in a direction opposite to the laser beam.

6. DISCUSSION OF RESULTS

Let us examine the self-focusing of the powerful laser beam in a medium near the focus of the lens.

In a low-intensity beam, the diameter of the focal spot d_0 is determined by the diffraction:

$$d_0 = 2\lambda_0 R / \pi a n_0,$$

where λ_0 is the wavelength of the light in vacuum, R and a are the radii of curvature and of the transverse cross section of the beam at the entrance to the nonlinear medium, and n_0 is the refractive index of the medium. The focal diameter of the powerful laser beam will be decreased by self-focusing.

The propagation of an intense beam in a medium with an instantaneous nonlinearity response, whose refractive index n increases in the field of the light wave ($n = n_0 + n_2 E^2$), was analyzed in^[9-11] by solving the wave equation in the quasioptical approximation. From this solution we can obtain an equation for the dimension of diameter δ with allowance for diffraction^[9]:

$$\frac{d^2\delta}{dz^2} = -\frac{1}{R_{nl}^2\delta^3} + \frac{1}{R_d^2\delta^3}, \quad (1)$$

where z is the coordinate along the beam axis, $R_{nl} = (1/2)a\sqrt{n_0/n_2}E^2$ and $R_d = ka^2/2$ are the wave-front curvature radii connected with the nonlinear refraction and with the diffraction, respectively, and k is the wave vector. At the entrance to the nonlinear medium we have $\delta(z) \equiv \delta(0) = 1$. The integral in Eq. (1) is^[9]

$$\left(\frac{d\delta}{dz}\right)^2 = \frac{1}{\delta^2} \left(\frac{1}{R_{nl}^2} - \frac{1}{R_d^2} \right) + C, \quad (2)$$

$$C = \frac{1}{R^2} - \frac{1}{R_{nl}^2} + \frac{1}{R_d^2}.$$

Putting

$$1/R_d^2 - 1/R_{nl}^2 = 1/R_{dn}^2, \quad (3)$$

we rewrite (2) in the form

$$\left(\frac{d\delta}{dz}\right)^2 = -\frac{1}{\delta^2 R_{dn}^2} + \frac{1}{R^2} + \frac{1}{R_{dn}^2}. \quad (4)$$

Unlike^[9], where the case $R_{nl} < R_d$ is considered (the beam power is larger than critical), we consider the behavior of the beam when $R_{nl} > R_d$, or when the power of the beam P is lower than critical P_{cr} . In this case self-focusing leads to a decrease of the diameter of the focal spot compared with the diffraction diameter d_0 . Let us find the minimal dimension of the beam d , by equating the derivative $d\delta/dz$ to zero:

$$\frac{1}{\delta^2} = 1 + \frac{R_{dn}^2}{R^2} \approx \frac{R_{dn}^2}{R^2}. \quad (5)$$

The approximate equation (5) is valid for a medium with low nonlinearity.

It follows from (3) that

$$R_{dn} = R_{nl} \left(\frac{P_{cr}}{P} - 1 \right)^{-1/4}, \quad (6)$$

$$P_{cr} = \lambda_0^2 c / 32\pi^2 n_2. \quad (7)$$

Substituting (6) and (7) in (5), we obtain the dependence of the focal diameter d on the radiation power:

$$d = d_0 (1 - P/P_{cr})^{1/4}. \quad (8)$$

With increasing radiation power, the diameter d decreases until the power density at the focus reaches the threshold value I_{thr} sufficient to damage the given material¹⁾. Using (8), we find the dependence of the threshold power P_{thr} on the focal diameter d_0 :

$$P_{thr} = \frac{d_0^2 I_{thr}}{1 + d_0^2 I_{thr}/P_{cr}}, \quad (9)$$

where $I_{thr} = 4P_{thr}/\pi d^2$.

If the term $d_0^2 I_{thr}/P_{cr}$ in the denominator of (9) is small compared with unity, the compression of the beam at the focus as a result of the self-focusing is negligible, and self-focusing does not play an important role in the damage of the material. This takes place when the radiation is focused with a short-focus lens into a sample with a low damage threshold and with low nonlinearity.

If $d_0^2 I_{thr}/P_{cr} \gg 1$, then $P_{thr} \approx P_{cr}$, and d is much smaller than d_0 as a result of self-focusing.

Thus, in order to observe experimentally the strong compression of the beam, it is necessary to choose a lens with maximum possible focal distance (maximum d_0) and a material with maximum nonlinearity (i.e., with the smallest value of P_{cr}). In our experiments the maximum nonlinearity was possessed by ZhS-11 glass. Using a lens with $f = 40$ cm, we observed contraction of the laser beam preceding the filamentary damage (Fig. 3).

Let us employ the obtained expressions for the interpretation of the experimental results. It should be borne

¹⁾Since we do not consider a concrete damage mechanism, we assume that the damage threshold is determined by the power density (or energy density) of the laser radiation.

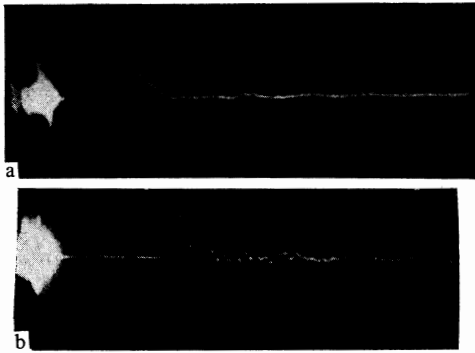


FIG. 7. Oscillograms of laser pulse scattered by a developing filamentary-like flaw: a – scattering by the entire filament, b – scattering by the end of the filament.

in mind here that the theory does not take into account the experimentally observed inertia of the nonlinearity.

Figure 4 shows the solid curves describing the dependence of P_{thr} on d_0^2 in accordance with expression (9). The values of I_{thr} and P_{cr} are the parameters of these curves. The curves were plotted for the following values of I_{thr} and P_{cr} : 1.3×10^{10} W/cm² and 1.5×10^5 W for ZhS-11 glass, 2.5×10^{10} W/cm² and 5×10^5 W for sapphire, and 3×10^2 W/cm² and 7×10^5 W for K-8 glass. The values of I_{thr} and P_{cr} can be determined by writing (9) in the form

$$I_{meas}^{-1} = I_{thr}^{-1} + d_0^2/P_{cr} \quad (10)$$

(where $I_{meas} = 4P_{thr}/\pi d_0^2$), and by plotting the experimental curve of I_{meas}^{-1} against d_0^2 . Then the intersection of the experimental lines with the ordinate axis, as follows from (10), gives the value of I_{thr}^{-1} , and the slope relative to the abscissa axis gives P_{cr}^{-1} . The values of P_{cr} and the corresponding values of n_2^{cr} are listed in the table.

It is seen from Fig. 4 that the experimental results are well described by expression (9) for ZhS-11 glass and sapphire. However, for K-8 glass at $d_0 > 5 \times 10^{-3}$ cm, the experimental values of P_{thr} increase with d_0^2 more strongly than would follow from (9). This discrepancy may be connected with the fact that P_{cr} increases in this region like $\sim d_0^2$. The reason for the dependence of P_{thr} on d_0 will be considered below.

The most probable mechanisms of self-focusing in solid dielectrics may be connected with thermal effects and with electrostriction. According to Litvak^[12], heating of a medium in the light channel can lead to self-focusing, if the refractive index of the medium increases with temperature (i.e., $dn/dT > 0$). Sapphire and glass are substances of this kind. A characteristic feature of thermal self-focusing is the dependence of n_2 on the time t and on the absorption coefficient κ . The experimentally observed decrease of the threshold P_{thr} for the formation of self-focusing filaments with increasing absorption for sapphire and ZhS-11 glass shows that self-focusing in these materials is determined by the thermal mechanism.

The value of P_{cr} calculated in accordance with^[12] is 2.5×10^5 W for sapphire with $\kappa = 2 \times 10^{-2}$ cm⁻¹ and 0.7×10^5 W for ZhS-11 glass. These values are approximately half the values of P_{cr} calculated from the ex-

perimental data using expression (10). Taking into consideration the approximate character of the stationary theory, from which expression (10) is derived, we can regard the agreement between the calculated and experimental values as satisfactory. The differences between the calculated values of P_{cr} and the experimental ones may be connected also with the large relaxation time of the excited states, compared with the duration of the pulse, and with the saturation of the absorption. We note that for thermal self-focusing the increment of the refractive index increases with time and reaches a maximum at the end of the pulse. The values of n_2 estimated from experiment pertain to the second half of the laser pulse, when the power density at the focus reaches a maximum.

In K-8 glass, where the absorption coefficient is small ($\kappa \approx 10^{-3}$ cm⁻¹), an important role may be played, besides the thermal mechanism, also by the mechanism of electrostriction, which was considered in^[13]. The striction self-focusing can be regarded as a stationary process, if a quasiequilibrium density of matter, corresponding to the striction pressure produced in the light field, is established in the light channel during the time of the laser pulse. The nonlinear increment n_2 of the refractive index, calculated in accordance with^[13], amounts to 1.5×10^{-14} cgs esu, while the thermal effects yield $n_2 \approx 1.0 \times 10^{-14}$ cgs esu. The critical power determined by the joint action of the striction and thermal mechanisms amounts to 9×10^5 W, which is close to the experimental 7×10^5 W. If the beam diameter at the focus is $d_0 > 5 \times 10^{-3}$ cm, then the density of the matter in the channel does not reach the equilibrium value during the pulse time τ_{pulse} , since $d_0 > \tau_{pulse}v_{ac}$ (v_{ac} – velocity of sound in the medium). In this case it is necessary to take into account the nonstationary character of the striction self-focusing, which leads to a dependence of the critical power on the beam diameter. According to^[13], $P_{cr} \sim d_0^2$. This apparently explains the deviation of the dependence for the K-8 glass in Fig. 4 from the calculated value at a diameter $d_0 > 5 \times 10^{-3}$ cm, starting with which P_{cr} increases approximately quadratically with increasing d_0 .

The possible action of the striction mechanism of self-focusing in K-8 glass is qualitatively confirmed also by the appearance in this glass of stimulated Mandel'shtam-Brillouin scattering at a power approximately half as large as the threshold of the filamentary damage (for a focusing lens with $f = 10$ cm). This is evidence of the appreciable value of the constant $(\rho \partial \epsilon / \partial \rho)$ for glass, which determines also the threshold of the striction self-focusing^[13]. At the same time, we were unable to observe stimulated scattering in sapphire crystals, at a radiation power 4–5 times larger than the threshold of filamentary damage.

Let us examine now the development of filamentary damage during the time of the laser pulse at a radiation power exceeding the threshold. At the first instant, the collapse of the beam occurs in the focal region of the lens, where the filamentary damage is initiated. The subsequent increase of the radiation power leads to an increase of the refractive index of the medium and to a decrease of the self-focusing length. The region of collapse moves in a direction opposite to the incident beam. The position of the end of the filamentary flaw is

determined by the maximum value of the increment Δn of the refractive index of the medium. For inertialess self-focusing, the maximum value of Δn is reached at the maximum of the laser pulse. In the case of mechanisms with inertia, on the other hand, the maximum of Δn can lag the pulse maximum.

The length of the filamentary flow is determined thus as the difference between the focal distance of the lens in the sample z_f , where the filament-like damage begins, and the minimum length of self-focusing z_{sf} which determines the position of the end of the filament.

In accordance with^[9] we have

$$1/z_{sf} = 1/R_{nd} + 1/|R|, \quad (11)$$

where

$$R_{nd} = R_{nl} (1 - P_{cr}/P)^{-1/2}, \quad z_f = |R|.$$

Then the length of the filament is $L = z_f - z_{sf} = R^2/(|R| + R_{nd})$. For the case $R_{nd} \gg |R|$, we get

$$L = 4\sqrt{2} \left(\frac{n_2}{cn_0^2} \right)^{1/2} \left(\frac{R}{a} \right)^2 (P - P_{cr})^{1/2}. \quad (12)$$

The inequality $R_{nd} \gg |R|$ corresponds to small changes of the focal distance of the lens due to the self-focusing, compared with the focal distance itself.

We note that z_{sf} determines the position of the collapsed region, where the beam diameter d vanishes. At the same time, from the preceding analysis it follows that filamentary damage occurs when $d > 0$. We take this circumstance into account by writing in place of (12) an approximate equation, in which P_{cr} is replaced by P_{thr} :

$$L \approx 4\sqrt{2} \left(\frac{n_2}{cn_0^2} \right)^{1/2} \left(\frac{R}{a} \right)^2 (P - P_{thr})^{1/2}. \quad (13)$$

The filament length L , as follows from experiment (Fig. 5), depends linearly on $(P - P_{thr})^{1/2}$ in accordance with (13). From the slopes of the lines we determine the values of n_2 for the investigated materials. These values, which are listed in the table, are in satisfactory agreement with the values of n_2 obtained from the threshold experiments.

We note once more that the foregoing analysis, as well as the analysis of the results of the threshold

measurements, is based on a stationary self-focusing theory, in which n_2 is a constant of the material and does not depend on the spatial coordinates or on the time. For real nonstationary processes, this analysis is approximate. At the same time, satisfactory agreement between the foregoing analysis and the experimental results offers evidence that the inertia of the nonlinearity does not change radically the course of the self-focusing in solids

In conclusion, we are grateful to T. N. Mikhaïlova for help with the work.

¹G. A. Askar'yan, Zh. Eksp. Teor. Fiz. 42, 1567 (1962) [Sov. Phys.-JETP 15, 1088 (1962)].

²V. P. Talanov, Izv. Vuzov Radiofizika 7, 564 (1964).

³R. Chiao, E. Garmire, and C. Townes, Phys. Rev. Lett. 13, 479 (1964).

⁴S. A. Akhmanov, A. P. Sukhorukov, and R. V. Khokhlov, Usp. Fiz. Nauk 93, 19 (1967) [Sov. Phys.-Uspekhi 10, 609 (1968)].

⁵M. Hercher, J. Opt. Soc. Amer. 54, 563 (1964).

⁶G. M. Zverev, T. N. Mikhaïlova, V. A. Pashkov, and N. M. Solov'eva, ZhETF Pis. Red. 5, 391 (1967) [JETP Lett. 5, 319 (1967)].

⁷G. M. Zverev, E. A. Levchuk, and É. K. Maldutis, and V. A. Pashkov, Fiz. Tverd. Tela 11, 1060 (1969) [Sov. Phys.-Solid State 11, 865 (1969)].

⁸G. M. Zverev, É. K. Maldutis, and V. A. Pashkov, ZhETF Pis. Red. 9, 108 (1969) [JETP Lett. 9, 61 (1969)].

⁹S. A. Akhmanov, A. P. Sukhorukov, and R. V. Khokhlov, Zh. Eksp. Teor. Fiz. 50, 1537 (1966) [Sov. Phys.-JETP 23, 1025 (1966)].

¹⁰P. Kelley, Phys. Rev. Lett. 15, 1005 (1965).

¹¹V. I. Bespalov and V. I. Talanov, ZhETF Pis. Red. 3, 471 (1966) [JETP Lett. 3, 307 (1966)].

¹²A. G. Litvak, *ibid.* 4, 341 (1966) [4, 230 (1966)].

¹³Yu. P. Raizer, Zh. Eksp. Teor. Fiz. 52, 470 (1967) [Sov. Phys.-JETP 25, 308 (1967)].

Translated by J. G. Adashko